Role of particle size and gas pressure on the nonlinear oscillatory behavior of a dust particle in a direct current discharge

S. Park, C. R. Seon, and W. Choe[a)]
Department of Physics, Korea Advanced Institute of Science and Technology, 373-1 Guseong-dong, Yuseong-gu, Daejeon 305-701, Korea

(Received 22 June 2004; accepted 9 August 2004; published online 18 October 2004)

Experimental and theoretical studies were conducted to simultaneously study the role of particle size and gas pressure on nonlinear behavior of dust oscillations in a plasma. Oscillation spectra were experimentally obtained by using four different sized (1.5, 2, 3, and 4 μm) particles at 250 mTorr, which is high pressure compared to previously reported works. The measured results were in good agreement with theoretical calculations based on a self-consistent collisional plasma model and a parametric dust oscillation model. In addition, particle size and gas pressure dependence of force profile and oscillation spectrum was investigated by numerical calculation in order to understand the role of particle size and pressure separately. It is concluded that occurrence of the subharmonic resonance and the net trapping force profile are mainly determined by particle size while gas pressure is mostly responsible for the superharmonic resonance and hysteresis. © *2004 American Institute of Physics*. [DOI: 10.1063/1.1801911]

I. INTRODUCTION

Dust particles introduced into a plasma are charged by incident electrons and ions. The charged dust particles experiencing various forces such as gravity, electrostatic force, ion drag force, etc., are likely to be localized or trapped around the plasma-wall boundary where force balance is achieved. The trapped particles often show oscillations induced by themselves[1–3] or by external drive.[4] The oscillatory motion of the particles is not only important for understanding the dynamics of particles in plasma but it can also be utilized for diagnosing particles and plasmas. For instance, it was attempted to determine particle charge assuming parabolic sheath potential[5–7] and to measure electrostatic potential based on the anharmonic forced oscillator model of a vertically oscillating particle in the radio-frequency (rf) sheath.[4]

Recent studies on forced oscillations of (4–10) μm sized particles at relatively low pressure (<80 mTorr) reported observation of nonlinear features, such as secondary resonance, hysteresis, and amplitude-dependent frequency shift of resonance peaks, where the crucial factors for determining the nonlinear oscillation were also investigated.[4,8,9] Possible causes of the nonlinear phenomena include nonlinearity of the trapping forces, spatial dependence of the driving force and charge, and low frictional damping due to low gas pressure.[9] Although the contribution from each factor differs in various situations, the most important factors seem to be gas pressure that determines damping rate of oscillatory motion and nonlinearity of the trapping forces. On the other hand, the nonlinear phenomena in the oscillatory particle motion have been difficult to observe at high pressure, since not only is the damping rate high but also the electric field in the vicinity of the trap position is known to be linear with spatial coordinate.[7] In the case of small particle size, however, the aforementioned arguments on the nonlinear oscillations may lead to a different result. For small-sized particles (1–2 μm radius), the electrostatic force and the ion drag force become much larger than the gravitational force, so that particle trapping occurs at the presheath region where the electrostatic force and the ion drag force are still nonlinear even at relatively high pressure. This work was motivated by an experimental observation of nonlinear oscillatory phenomena with small-sized (1.5 μm radius) particles at relatively high pressure 250 mTorr which seemed rather exceptional based on the previous works. The observation suggested that the origin of the nonlinear behavior of dust oscillation should be studied in a more refined manner. In order to achieve the goal, investigation about the separate role of particle size and pressure on the nonlinearity of dust oscillation was attempted through measurement and modeling, and the results are presented.

II. EXPERIMENTAL SETUP

Experiments were performed using a cylindrical dc plasma source as shown in Fig. 1. The plasma source consisted of a cathode of 8 cm diameter placed at the bottom and a center-holed anode (outer diameter=11 cm, inner diameter=6 cm) placed at the top. The distance between the anode and the cathode was 6 cm. A dust dispenser and an excitation wire were inserted into the chamber. The dust dispenser made of a simple beep speaker was used to introduce dust particles. In this work, four different sized (1.5, 2.0, 3.0, and 4.0 μm radius) monodisperse particles were used. The 1.5 μm sized particle was made of SiO_2 (mass density $=2.2\ g/cm^3$), and the other three types were made of melamine formaldehyde (MF, mass density$=1.5\ g/cm^3$). A patch of fine tungsten wire of 0.2 mm diameter used as an excitation wire was located at 24 mm above the cathode, and it was connected to a function generator for providing an alternating current (ac) voltage. To confine particles toward

[a)]Electronic address: wchoe@kaist.ac.kr

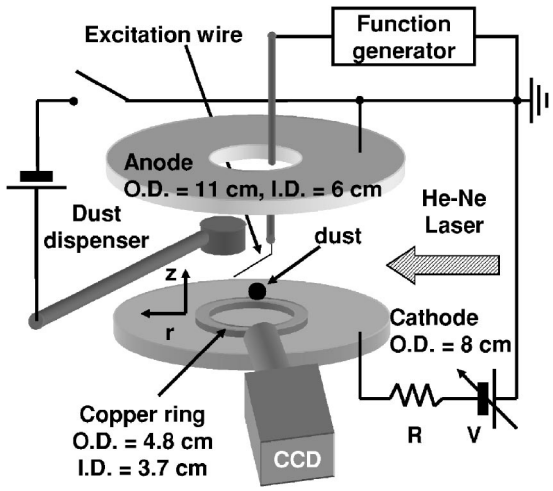

FIG. 1. Schematic diagram of the experimental setup.

the radial center, a copper electrode (outer diameter =4.8 cm and inner diameter=3.7 cm) was placed on the cathode. A typical glow discharge was produced at the cathode voltage of $V_c=-320$ V and current of $I_p=1$ mA with argon gas feeding at 250 mTorr. The injected 1.5 μm radius SiO_2 particles were trapped at about 10 mm above the cathode surface. Measurements of the trapped dust oscillation amplitude were conducted by forward and backward frequency sweep of the ac voltage with 0.5 Hz step frequency on the excitation wire. For visualization and recording of the oscillation trajectories, a light scattering method was implemented using a 632.8 nm He-Ne laser. The scattered light intensity was recorded using a set of zoom lens, charge-coupled device (CCD) detector, and a general video capture board. To extract oscillation amplitude from the captured movie containing particle trajectories, a home-made image processing software was utilized.

III. PLASMA-SHEATH MODEL, CHARGING, AND EXERTED FORCES

In order to model the dust oscillatory motion, a proper plasma-sheath model and careful evaluation of the forces exerted on a dust particle are required. In the case of a small-sized dust particle, it is likely to be trapped in the subsonic region where charge neutrality is nearly valid and ions have rather slow subsonic fluid velocity; thus a plasma-sheath model should be capable of dealing with the presheath region as well as the sheath region. At relatively high pressure, ion-neutral collisions should also be taken into account. With the above fact being considered, the plasma-sheath modeling was done by solving a set of equations expressed as[10–12]

$$n_i u_i = n_0 u_B \equiv \text{const}, \tag{1}$$

$$n_e = n_0 \exp\left(\frac{e\phi}{kT_e}\right), \tag{2}$$

$$m_i n_i u_i \frac{du_i}{dz} = -n_i e \frac{d\phi}{dz} - m_i n_i \frac{\pi}{2\lambda_i} u_i^2, \tag{3}$$

$$\epsilon_0 \frac{d^2\phi}{dz^2} = -e(n_i - n_e), \tag{4}$$

where n_i, n_0, u_i, u_B, ϕ, m_i, T_e, k, and λ_i denote ion density, electron density at $u_i=u_B$, ion fluid velocity, Bohm velocity, electrostatic potential, ion mass, electron temperature, Boltzmann constant, and ion mean free path, respectively. z is the vertical coordinate from the cathode surface toward the bulk plasma. For boundary conditions, the quasineutral limit ($n_e=n_i$) solution of Eqs. (1)–(4) was utilized. Since it is expressed as an analytic function of z, plasma potential ϕ, u_i, and n_i can be easily evaluated at sufficiently distant position from the sheath, i.e., at the bulk plasma where the quasineutral solution is valid.[10] It provided good starting values for the fourth-order Runge-Kutta integration from the bulk plasma to the cathode. In addition, experimental values were used for other parameters such as T_e, n_0, and λ_i, obtained from probe and pressure measurements.

The particle charge and the forces were self-consistently evaluated from the plasma model. To evaluate the dust charge, the orbital-limited motion (OML) theory of a spherical probe was applied with considering ion thermal motion:[13]

$$n_i \sqrt{u_i^2 + \frac{8kT_i}{\pi m_i}} \left\{ 1 - \frac{Qe}{2\pi\epsilon_0 a m_i \left(u_i^2 + \frac{8kT_i}{\pi m_i} \right)} \right\} - n_e \sqrt{\frac{8kT_e}{\pi m_e}} \exp\left(\frac{Qe}{4\pi\epsilon_0 a k T_e} \right) = 0, \tag{5}$$

where Q and a denote the dust charge and radius, respectively. It is pointed out that the charge is underestimated at subsonic region ($u_i<u_B$) if the ion thermal motion is ignored.

For force calculation, the gravitational force and the friction coefficient η of the neutral drag force[14] were directly evaluated from the size and mass density of the dust particle, the gas pressure, and the gas temperature. The friction coefficient was also measured using the same method as in Ref. 15 by fitting small oscillation spectrum to Lorentzian.

The electrostatic force and the ion drag force were evaluated using the particle charge obtained by solving Eq. (5). While the electrostatic force can be easily evaluated as charge multiplied by electric field, evaluation of the ion drag force needs more consideration. In general, the ion drag force is formulated as the following:

$$\mathbf{F}_{id} = m_i n_i \int \mathbf{v} v f_i(\mathbf{v}) \{\sigma_c(v) + \sigma_s(v)\} d^3 v, \tag{6}$$

where $\mathbf{v}$, $f_i(\mathbf{v})$, $\sigma_c(v)$, and $\sigma_s(v)$ are ion velocity, ion velocity distribution function, collection cross section, and orbital cross section, respectively.[13,16,17] In the case of low pressure collisionless plasma, ions are usually approximated to be monoenergetic because a dust particle is likely to be trapped in the supersonic ion resident region. However, in the case of relatively high pressure collisional plasma, the dust particle is rather trapped at the subsonic region, and thus ion velocity distribution is rarely monoenergetic but drift-Maxwellian. For the orbital cross-section formula, Ref. 17 reported a

modification of that of Refs. 13 and 16, but it produced just a little correction of the ion drag force in our work. From the above consideration and the scattering cross section given in Ref. 17, the ion drag force of the drift-Maxwellian ions is expressed as

$$F_{id}(u_i) = n_i m_i \sqrt{\pi} a^2 v_t^2 \int_0^\infty du \frac{e^{-(u^2+u_0^2)}}{u_0^2} \times [2u_0 u \cosh(2u_0 u) - \sinh(2u_0 u)] \times \left[u^2 + 2\epsilon + 4\frac{\epsilon^2}{u^2} \ln \frac{1+\delta^{-2}(u^4+2\delta u^2)}{1+\epsilon^{-2}(u^4+2\epsilon u^2)} \right], \quad (7)$$

where $u_0 \equiv u_i/v_t$, $v_t \equiv \sqrt{2kT_i/m_i}$, $\epsilon \equiv Qe/4\pi\epsilon_0 m_i v_t^2 a$, $\delta \equiv Qe/4\pi\epsilon_0 m_i v_t^2 \lambda_D$, and λ_D is the screening (Debye) length of the plasma, respectively.

IV. DUST VERTICAL OSCILLATION MODEL

Assuming no flow and no temperature gradient of neutral gas, the equation of motion of a dust particle parametrically driven inside plasma in the vertical direction perpendicular to the cathode can be expressed as

$$\frac{d^2z}{dt^2} = -\frac{\eta}{m_d}\frac{dz}{dt} + \frac{1}{m_d}F_{es}[z;V_{exc}(t)] + \frac{1}{m_d}F_{id}[z;V_{exc}(t)] + g, \quad (8)$$

where m_d is the dust mass, η is the friction coefficient of the neutral drag force, F_{es} and F_{id} are the electrostatic force and the ion drag force, respectively. $V_{exc}(t) = V_m \sin(2\pi ft)$ is the ac voltage applied to the excitation wire where f denotes the driving frequency. Sorasio *et al.* (Ref. 18) introduced a model for nonlinear dust parametric oscillation based on polynomial representation of the trapping force in position, in which the displacement of the trapped particle was assumed to be sinusoidal in time. However, the vertical displacement induced by the excitation voltage was not sinusoidal in time in our experiment, and the measured frequency shift of the resonance peaks in the oscillation spectrum was larger than the value obtained from the model. Because of the reasons, Eq. (8) was directly solved numerically in this work by evaluating the net force with time-varying excitation voltage V_{exc} at each time step.

In many previous works where dust oscillations were induced by imposing an ac applied voltage to the excitation wire located above the cathode or rf electrode, the ac voltage application appeared to make little effect on plasma. As a result, it was considered that the applied voltage provided pure forced oscillations on a dust particle. However, Ref. 19 pointed out that the ac voltage application could induce plasma density modulation which in turn gives rise to a parametric particle oscillation in addition to the forced oscillation. In our experimental condition, on the other hand, the ac excitation turned out to induce a strong parametric oscillation which was confirmed by calculation as well as measurement of dust trap position, plasma current, and density as described below.

The plasma density modulated by the wire excitation $[V_{exc} = V_m \sin(2\pi ft)]$ was measured by a Langmuir probe at $z = 35$ mm, which was nearly the bulk plasma region. The fractional density variation was fitted as $\tilde{n}_p/n_p \simeq 1.04 \times 10^{-2} V_{exc} + 6.36 \times 10^{-4} V_{exc}^2$, where $\tilde{n}_p$ is the difference between the plasma density at V_{exc} and the nonperturbed plasma density n_p at $V_{exc} = 0$. For example, $\tilde{n}_p/n_p \simeq 7\%$ at $V_{\rm exc} = 5$ V. The fractional ion density variation ($\tilde{n}_i/n_i$ due to the ac voltage application was also calculated as a function of z by integrating Eqs. (1)–(4) using the aforementioned empirical formula on $\tilde{n}_p/n_p$. The result showed that the ac application induces strong position-dependent density modulation. As shown in Fig. 2, $\tilde{n}_i/n_i$ becomes very large (up to about 75%) just below the trap position and the tendency was similarly seen in electron density. It is noted that $\tilde{n}_i$ was defined as the difference between $n_i(V_{exc})$ and $n_i(V_{exc}=0)$ in the same manner as $\tilde{n}_p$. The plasma parameters, potential, dust charge, and various forces the particle were calculated successively in time using the measured bulk plasma density $n_p + \tilde{n}_p(V_{exc})$ and the plasma model described in the preceding section.

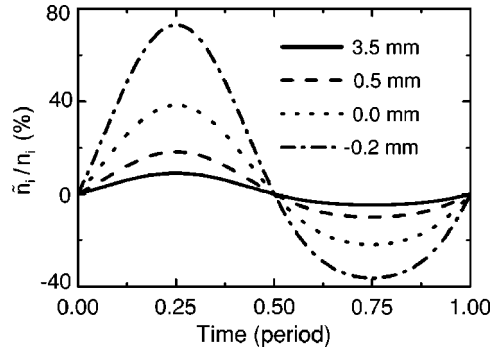

FIG. 2. Calculated fractional ion density variation ($\tilde{n}_i/n_i$) at four different locations near the trap position (0 mm) due to an ac voltage application on the excitation wire, $V_{exc} = 5.0 \times \sin(2\pi ft)$ ($V_m = 5.0$ V). The locations 3.5 mm and −0.2 mm in the plot denote 3.5 mm above and 0.2 mm below the trap position, respectively. This calculation was based on the measured plasma density at 25 mm above the trap position.

V. RESULTS AND DISCUSSIONS

Figure 3(a) shows the measured frequency spectra of the vertical dust oscillation at 10 different excitation voltages at 250 mTorr which is high pressure compared to the previous studies. For small amplitude oscillations ($V_m = 1.0$ V), a Lorentzian spectrum of the linear forced oscillation is seen. It has a single primary resonance peak at 54 Hz, which is considerably higher than that in the previously reported experiments.[4,8,9,18–20] The high resonance frequency can be attributed to the small mass of the small-sized dust particle ($a = 1.5$ μm). Another feature of the spectrum is its large full width at half maximum (FWHM), and it reflects high damping rate by high gas pressure. At larger V_m, nonlinear features began to be observed. Above 2.0 V, the superharmonic resonance peak appeared at about half of the primary resonance frequency. In addition, the resonance peak downshifted as V_m was increased. At further larger V_m over 8.0 V, the subharmonic resonance appeared at about twice of the primary resonance frequency. Finally, hysteresis was observed at the primary and the subharmonic resonance peaks. Figures 3(b)

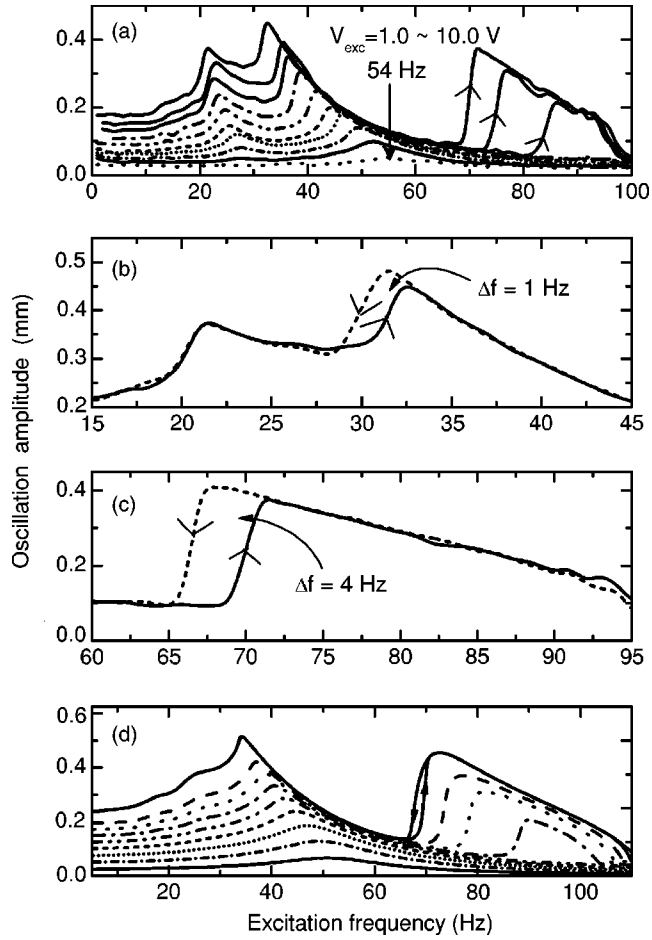

FIG. 3. (a) Measured spectra of the vertical dust oscillation at ten different excitation ac voltages $V_m=(1.0-10.0)$ V with 1.0 V step during forward frequency sweep. Detailed view of the measured spectra during forward and backward frequency sweep around (b) the primary and (c) the subharmonic resonance peak where $V_m=10.0$ V. For the experimental conditions, $a=1.5$ μm, p=250 mTorr, $V_c=-320$ V, $I_p=1$ mA, $n_p \simeq 5\times 10^9$ cm^{-3}, $kT_e \simeq 1$ eV, and the step frequency was 0.5 Hz. Dust particles were trapped at 10 mm above the cathode surface. (d) Calculated spectra with the same plasma density, electron temperature, and particle size as (a) at 250 mTorr. The primary resonance frequency $f_0=52$ Hz and $V_m=(1.0-8.0)$ V.

and 3(c) show an example at 10.0 V of which hysteresis frequency difference is 1 Hz and 4 Hz, respectively. In summary, the experimental observations demonstrate that the frequency dependence of the dust oscillation at 250 mTorr has similar characteristics as those at lower pressure.

The experimental results at the high pressure are consistent with the following results of the numerical modeling. Figure 3(d) shows a set of frequency spectra that were calculated based on the measured plasma density, electron temperature, gas pressure, particle size, and particle mass density as in Fig. 3(a). The calculations were conducted at eight different excitation voltages during the backward and the forward frequency sweep. Compared with Fig. 3(a), the calculated primary resonance frequency (52 Hz) agrees well with the measured value (54 Hz). Also, the nonlinear features such as amplitude-dependent frequency shift of the resonance peaks, occurrence of the secondary resonances, and the hysteresis around the resonance peaks show basically the same tendency as the experimental results except a little quantitative discrepancy. Both measurement and modeling assert the possibility of the nonlinear oscillatory behavior even at the high pressure, suggesting that the condition for nonlinear phenomena should be investigated by considering not only gas pressure but also particle size.

The experimental and theoretical results shown in Fig. 3 indicate that the wire does not act as an external driver because if this is the case, the subharmonic resonance peak would be generally much smaller than the primary resonance peak. On the other hand, the results clearly show that both the primary resonance and the subharmonic resonance are excited by the same excitation voltage, and they are comparable. As explained in Refs. 19 and 20, this behavior is induced by the fact that the trapping potential well oscillates as a result of the wire voltage modulation. In this oscillation, the wire excitation makes two types of resonance; the primary resonance induced by shaking the particle directly and the subharmonic resonance induced by modulating the trapping potential profile (parametric resonance).

Figure 4 shows the oscillation spectra depending on particle size at fixed pressure under the same plasma condition as that of Fig. 3. The spectra (a)–(c) were measured using 2 μm, 3 μm, and 4 μm particles, and the corresponding spectra (d)–(f) were calculated by modeling, respectively. Both spectra obtained by measurement and modeling present a distinctive size-dependent difference. The subharmonic resonance peak appears clearly with a 2 μm particle but not with larger particles, which means that oscillation of larger particles is more linear. It is pointed out that the difference originated solely from the different particle size because plasma condition and gas pressure were all same. As a result, it is found that the particle size is a key parameter to determine the occurrence of the subharmonic resonance peak.

As was mentioned in Sec. I, two requirements should be simultaneously satisfied for nonlinear features to be developed in dust oscillations which are low frictional damping and nonlinearity of the trapping force. In general, particle size affects both frictional damping and trapping force. η/m_d in the damping term in Eq. (8) is proportional to p/a because the neutral drag force ($\propto \eta$) is proportional to pa^2 (Ref. 14) and $m_d \propto a^3$, thus a larger particle has a smaller damping coefficient. It means that a larger particle experiences less frictional damping, and as a result, nonlinearity should be easier to be developed with a larger particle than with a smaller one. Figure 4, however, clearly shows the opposite tendency against the above argument by showing the occurrence of the subharmonic resonance with only smaller particles. This contradiction leads to the consideration of the force profile dependence on particle size.

Figure 5 shows the force profile corresponding to the spectra of Figs. 3(d) and 4(d)–4(f). As particle size becomes larger, the force profile in the vicinity of the trap position where $F_{\text{net}}=0$ becomes more linear, which was confirmed by the second or higher order coefficients of its polynomial representation. In addition, the overall shape of the force profile seems to be highly dependent on particle size. Based on the frequency spectrum measurement and calculation with different particle size, it is found that particle size is also an

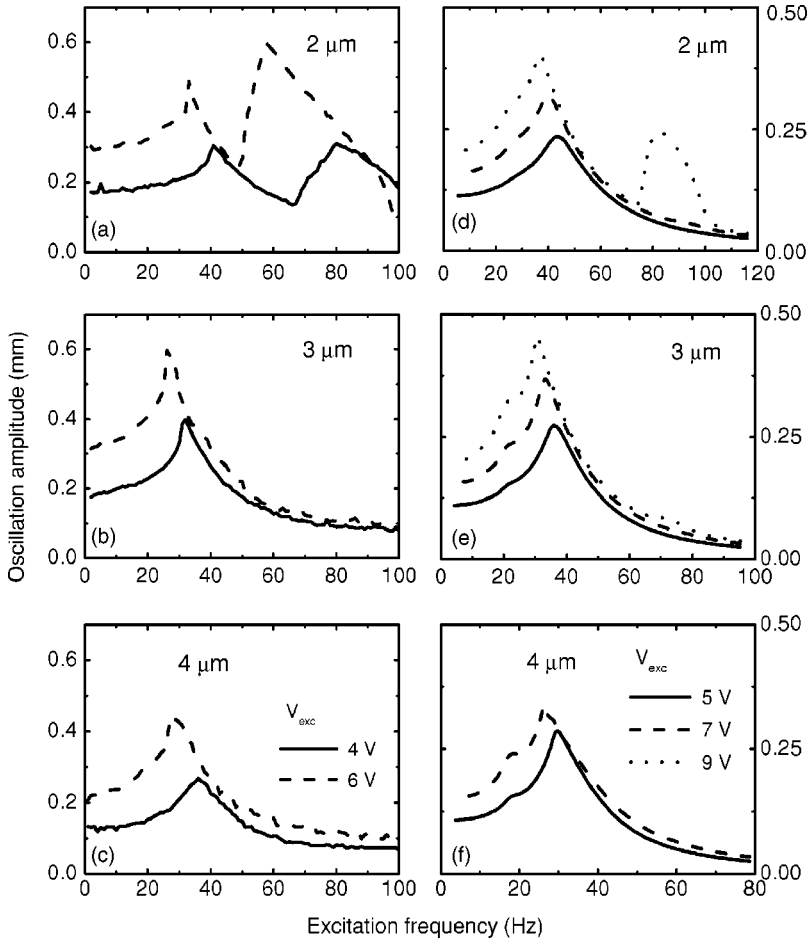

FIG. 4. The spectra (a–c) were measured with 2, 3, and 4 μm particles, respectively. The spectra (d–f) were obtained by modeling corresponding to the spectra (a–c). The numerical simulation was performed under the experimental condition where electron temperature and plasma density were 1.0 eV and 5×10^9 cm^{-3} at 250 mTorr, respectively.

important parameter in determining nonlinear features of dust oscillations.

In the following, further investigation of the role of particle size and gas pressure on oscillation characteristics was attempted by studying the frequency spectra versus particle size (1–4 μm) and gas pressure (50–400 mTorr) obtained by numerical simulation. In Fig. 6, the spectra at 50 mTorr were calculated with V_m=4.0 V, while the spectra at other pressure were calculated with V_m=6.0 V because the dust particle was no longer trapped due to its large oscillation amplitude if $V_m>4.0$ V at 50 mTorr. This figure enables us to understand the role of particle size and gas pressure separately, and the main findings are as follows. First, all the spectra at 400 mTorr show Lorentzian profile because of high damping due to high pressure. From the fact that a larger particle shows smaller FWHM, a larger particle is found to experience less frictional damping as previously discussed. Second, the superharmonic resonance appears regardless of particle size and gas pressure in all the spectra except at 400 mTorr although the detailed shape such as sharpness of the resonance peak slightly differs from each other. Third, it again confirms that the subharmonic peak shows rather larger dependence on particle size than on gas pressure. At 200 mTorr, the subharmonic peak appears only in the 1 μm and 2 μm cases, while it occurs in the 1 μm, 2 μm, and 3 μm cases at 100 mTorr. In the case of 4 μm, however, no spectrum showed subharmonic resonance regardless of gas pressure. Therefore, the results demonstrate that (1) nonlinear features can appear even at high pressure (~200 mTorr), (2) particle size is a main factor in occurrence of the subharmonic resonance, and (3) subharmonic resonance may not be developed even at low pressure if particle size is too large.

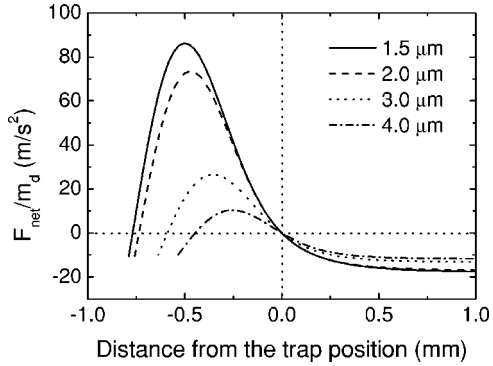

FIG. 5. Force profile of the four different sized particles obtained from Figs. 3(a) and 4(d)–4(f).

The following discussion on the force profile demonstrates that particle size affects the force profile more strongly than frictional damping. As plotted in Fig. 7 in which each spectrum is arranged in the same manner as that

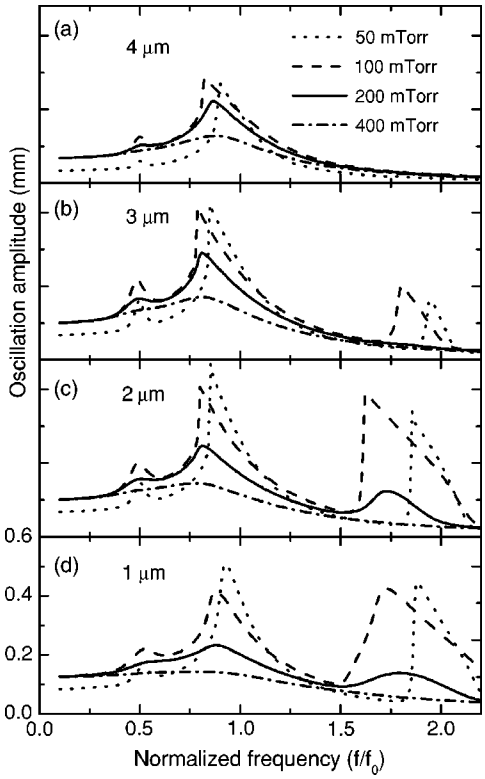

FIG. 6. Calculated oscillation spectra according to different particle size (1–4 μm) and gas pressure (50–400 mTorr); (a) $a=4.0$ μm, (b) $a=3.0$ μm, (c) $a=2.0$ μm, and (d) $a=1.0$ μm. Electron temperature and plasma density were set as 1.0 eV and 5×10^9 cm^{-3}, respectively. Only the spectrum at 50 mTorr of (a) was calculated with $V_m=2.0$ V, and the other spectra in (a) were calculated with $V_m=4.0$ V. The spectra at 50 mTorr of (b–d) were calculated with $V_m=4.0$ V, and the other spectra were calculated with $V_m=6.0$ V.

of Fig. 6, it is seen that the overall shape of the force profile mainly depends on particle size rather than gas pressure although higher gas pressure induces slightly steeper force profile. It means that the main difference in the oscillation spectra due to gas pressure results from different damping rate rather than different force profile although gas pressure affects the details. It also means that the difference of the oscillation spectra due to particle size at fixed pressure results from high size dependence of the trapping force profile.

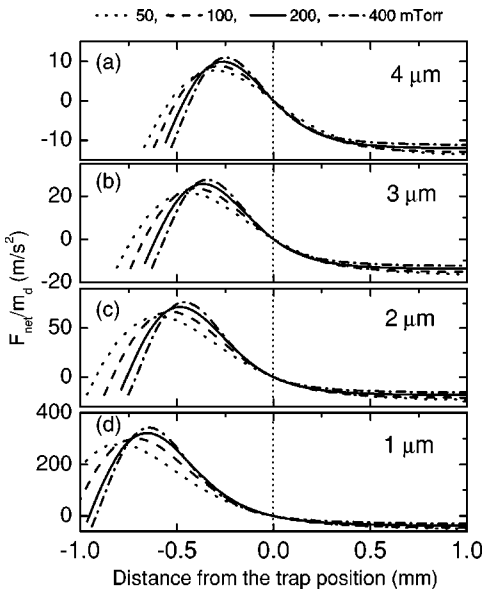

FIG. 7. Net force profile corresponding to the spectra of Fig. 6. Note that the range of the ordinate in (a–d) are different.

Since all the force profiles in Fig. 7 have some degree of nonlinearity, the overall characteristics such as height of each resonance peak, occurrence of the superharmonic resonance, etc., are also found to be determined by neutral damping rate that is a function of gas pressure. It is also noted that width of the hysteresis zone became smaller as the gas pressure was increased, which is consistent with studies at low pressure.[9] Whereas, particle size determines the characteristics of the subharmonic resonance that is related to the force profile as shown in Fig. 6.

Finally, it is mentioned that the "low gas pressure" is not a sufficient condition, but rather a necessary condition for the nonlinear features to be developed, and particle size plays an equally important role in the nonlinearity of dust oscillations.

VI. CONCLUSION

In this work, the parametric nonlinear oscillation of dust particles in a dc glow discharge at high pressure was investigated while focusing on the role of gas pressure and particle size. The full feature of the nonlinear oscillation at 250 mTorr was observed experimentally and it agreed well with the modeling result. The results suggest that gas pressure needs not to be very low for showing nonlinear features as previously reported, and particle size plays equally an important role in developing nonlinearity.

In order to demonstrate the role of particle size, size dependence of the frequency spectra was studied with three different size particles. From the measured result, it was found that occurrence of the subharmonic peak was highly dependent on particle size and the size determines the restoring force profile. The observations were consistent with modeling.

For further understanding, discussions about the role of particle size and gas pressure in nonlinear oscillations were made through numerical calculation of oscillation spectra and force profiles. It turned out that gas pressure affects the oscillation spectra by means of frictional damping rather than the overall net force profile, and the force profile is mainly determined by particle size rather than by gas pressure. Finally, it is concluded that occurrence of the subharmonic resonance and the force profile are mostly determined by particle size while the superharmonic resonance and hysteresis are determined by gas pressure through damping rate.

ACKNOWLEDGMENTS

The authors acknowledge the referee for his/her valuable comments. This work was partly supported by the Vacuum Center at Korea Research Institute of Standards and Science, partly by Korea Ministry of Science and Technology, and partly by Korea Basic Science Institute.

[1]S. Nunomura, T. Misawa, N. Ohno, and S. Takamura, Phys. Rev. Lett. **83**, 1970 (1999).
[2]A. A. Samarian, B. W. James, S. V. Vladimirov, and N. F. Cramer, Phys. Rev. E **64**, 0254021 (2001).
[3]D. P. Resendes, G. Sorasio, and P. K. Shukla, Phys. Plasmas **11**, 2394 (2004).
[4]A. V. Ivlev, R. Sutterlin, V. Steinberg, M. Zuzic, and G. Morfill, Phys. Rev. Lett. **85**, 4060 (2000).
[5]A. Melzer, T. Trottenberg, and A. Piel, Phys. Lett. A **191**, 301 (1994).
[6]H. Schollmeyer, A. Melzer, A. Homann, and A. Piel, Phys. Plasmas **6**, 2693 (1999).
[7]E. B. Tomme, D. A. Law, B. M. Annaratone, and J. E. Allen, Phys. Rev. Lett. **85**, 2518 (2000).
[8]C. Zafiu, A. Melzer, and A. Piel, Phys. Rev. E **63**, 066403 (2001).
[9]Y.-N. Wang, L.-J. Hou, and X. Wang, Phys. Rev. Lett. **89**, 155001 (2002).
[10]K.-U. Riemann, Phys. Plasmas **4**, 4158 (1997).
[11]K.-U. Riemann, J. Phys. D **36**, 2811 (2003).
[12]M. A. Lieberman and A. J. Lichtenberg, *Principles of Plasma Discharges and Materials Processing* (Wiley, New York, 1994), p. 170.
[13]M. S. Barnes, J. H. Keller, J. C. Forster, J. A. O'Neill, and D. K. Coultas, Phys. Rev. Lett. **68**, 313 (1992).
[14]P. S. Epstein, Phys. Rev. **23**, 710 (1924).
[15]B. Liu, J. Goree, V. Nosenko, and L. Boufendi, Phys. Plasmas **10**, 9 (2003).
[16]J.-P. Boeuf and C. Punset, in *Dusty Plasmas: Physics, Chemistry, and Technological Impact in Plasma Processing*, edited by A. Bouchoule (Wiley, New York, 1999), p. 34.
[17]S. A. Khrapak, A. V. Ivlev, G. E. Morfill, and H. M. Thomas, Phys. Rev. E **66**, 0464141 (2002).
[18]G. Sorasio, D. P. Resendes, and P. K. Shukla, AIP Conf. Proc. **649**, 239 (2002).
[19]G. Sorasio, D. P. Resendes, and P. K. Shukla, Phys. Lett. A **293**, 67 (2002).
[20]D. P. Resendes, G. Sorasio, and P. K. Shukla, Phys. Plasmas **9**, 2988 (2002).